CHAPTER II

THEORETICAL BACKGROUND AND LITERATURE REVIEW

2.1 Material Properties

2.1.1 Polyamide12 (Nylon12)

Polyamide12 (PA12 or Nylon12) is an engineering thermoplastic material produced by opening up a monomer containing both amine and acid groups known as a laurolactam ring as shown in Figure 2.1. Even though it is not as widely used as Nylon6 and Nylon66, the semicrystalline Nylon12 has physical properties that make it an excellent material for manufacturing many different products including cable jacketing, wire insulation, flexible hosing, flexible cover caps, damping cogwheels, protective coverings, nozzles, sheet gaskets, medical catheters, sealing rings, ski boots, automotive exterior parts, and even aircraft interior parts.
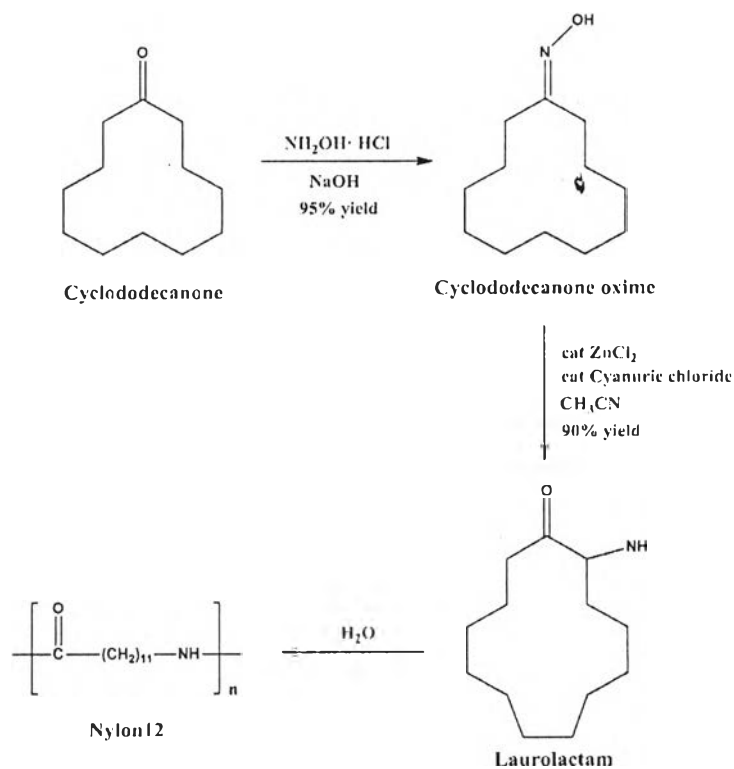

Figure 2.1 Preparation of Nylon12 via ring opening of a laurolactam.

Generally, the physical properties such as melting temperature (T_m) and water absorption of polyamides depend on the concentration of amide groups relating to the hydrogen bonds. The presence of a long hydrocarbon chain will lead to a reduced frequency of amide groups. With a lower concentration of amides (nitrogen-containing organic compounds) than any other commercially available polyamide as shown in Table 2.1, Nylon12's material characteristics make it beneficial in the following ways:

- It has low melting temperature. The melting points of polyamides can be explained on the basis of their relative ability to form hydrogen bonds. The more hydrogen bonding groups, the higher melting point of material is. The lower content of amide groups of Nylon12 as compared to Nylon6 limits the number of hydrogen bonds, and thus Nylon12 melts nearly 50 °C below Nylon6.

- It absorbs very little moisture. The association of water with amide groups is essentially a replacement of the amid-amide hydrogen bond with the amide-water hydrogen bond. Hence, low water absorption allows components made from Nylon12 to retain a high degree of dimensional stability, even in environments with fluctuating humidity levels.

- Even when temperatures dip below freezing, Nylon12 retains excellent impact and non-impact strength.

- It features excellent resistance to chemicals, including hydraulic fluids, oil, fuels, grease, salt water and solvents.

- Nylon12 has exceptionally strong resistance to cracking under stress, including instances when it encapsulates metal components.

- It provides excellent resistance to abrasion.

- When it is dry run against steel, polyacetal, polybutylene terephthalate (PBT) and other material, Nylon12 has a very low coefficient of friction.

- It dampens noise and vibration.

- Even when placed under high-frequency cyclical load, Nylon12 remains incredibly fatigue resistant.

- It is high processability.

Table 2.1 The relationship of the amide group concentration to melting temperature and water absorption with various types of polyamides (Chapman and Chruma, 1985)

Nylon Types	Amide Groups (%)	T_m (°C)	Water Absorption 24 h (%) ASTM D570
Nylon6,6	38	265	1.0-1.3
Nylon6	38	226	1.3-1.9
Nylon6,9	32	210	0.5
Nylon6,12	28	212	0.4
Nylon12	22	179	0.25-0.3

Nylons are linear aliphatic polyamides that are able to crystallize due to the presence of strong intermolecular hydrogen bonds through the amide groups of adjacent chains and Van der Waals forces between the methylene chains. These secondary bonding forces strongly affect to the chain conformation, the crystal morphology and the strength of Nylons. For crystal morphology, there are γ-phase and α-phase structures as shown in Figure 2.2 which the left side shows the view of the hydrogen-bonding planes, and the right side shows the view down the chain axis. The γ-phase crystallites are characterized as a triclinic structure that the chains are parallel and the hydrogen bonding is between chains in adjacent sheets. For the α-phase crystallites, they are characterized as a monoclinic structure that the adjacent chains are anti-parallel and the hydrogen bonding is between adjacent chains within the same sheet (bisecting the CH_2 angles).

For crystallization behavior of Nylon12, Northolt *et al.* (1972) observed that there were both monoclinic and triclinic structures. Many researches have shown that four different crystal forms are present in Nylon12: the γ-phase, γ'-phase, α-phase, and α'-phase. Mathias and Johnson (1991) reported on the various ways to obtain these different crystal forms. The γ-phase of Nylon12 is the most common thermodynamically stable form with a typical melting temperature of

179 °C (Aharoni, 1997; Li *et al.*, 2003). This phase is obtained upon cooling from the melt. The γ'-phase has been characterized as also being triclinic in structure with a longer periodicity than that seen in the γ-phase. It is obtained when the Nylon12 sample is quenched from the melt and has a melting temperature of 175 °C (Ishikawa *et al.*, 1980). Using DSC to observe the melting peaks, Mathias and Johnson (1991) also stated that the α-phase can only be obtained when the Nylon12 was produced from solution cast at low temperatures. These α-phase crystallites are characterized as being monoclinic in structure and having a melting temperature of 173 °C (Ishikawa *et al.*, 1980). The α'-phase has been observed by Li *et al.* (2003). They showed that this phase occurs at high temperatures and when the Nylon12 is crystallized at 175 °C. Generally, the α'-phase crystallites only exist at the elevated crystallization temperatures and disappear upon cooling. Upon cooling of the α'-phase from the elevated temperatures to the room temperature, Ramesh (1999) illustrated that the α'-phase crystallites of Nylon12 transform into the γ-phase, and it is the only polyamide that shows this behavior while other polyamides show the transformation of the α'-phase into the α-phase.

The orientation and crystallinity of Nylons strongly affect to mechanical, thermal and optical properties. Basically, higher molecular chain orientation and crystallinity will produce better properties. Crystallinity of nylons can be controlled by nucleation, i.e., seeding the molten polymer to produce uniform sized smaller spherulites. This results in increased tensile yield strength, flexural modulus, creep resistance, and hardness, but some loss in elongation and impact resistance.
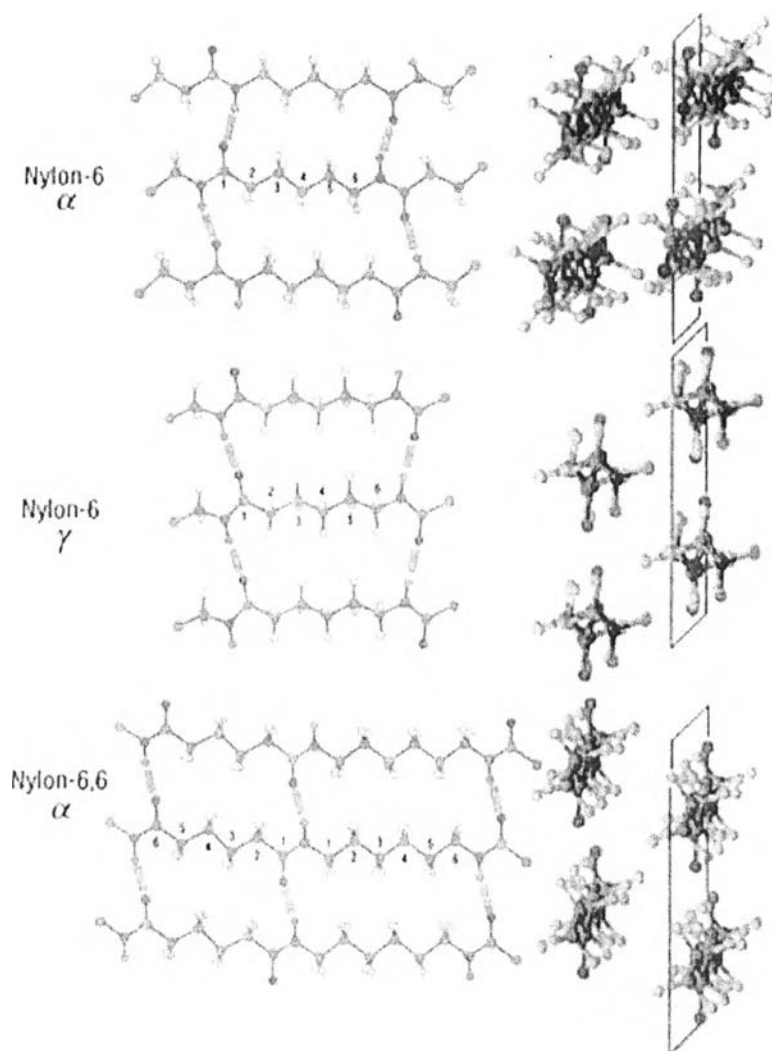
Figure 2.2 Crystal structures of σ-phase and γ-phase of Nylon6 and Nylon6,6 (Reprinted from Dasgupta *et al.*, 1996).

2.1.2 Natural Rubber

Natural rubber (NR) is an elastomer that is derived from latex, a milky colloid produced by certain plants and trees. NR latex is a natural polymer of isoprene (most often cis-1,4-polyisoprene as shown in Figure 2.3) obtained from the *Heavea Brasiliensis* tree. Typically, a small percentage (up to 5 % of dry mass) of other materials, such as proteins, fatty acids, resins and inorganic materials (salts) are found in NR. However, these substances can be removed when the latex is subjected to the manufacturing processes.
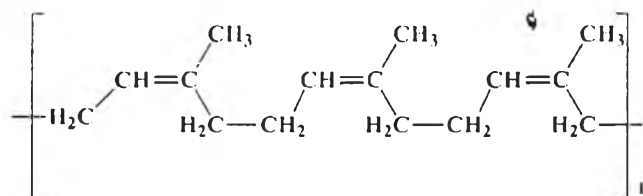
Figure 2.3 Chemical structure of cis-polyisoprene (main constituent of NR).

The most important forms in which NR is processed are the following: preserved latex concentrates, sheets, crepes, and block rubber. For preserved latex concentrates, NR latex is either preserved with ammonia or mixture of ammonia, zinc oxide and tetramethylthiuram disulfide (TMTD) for preventing the bacterial growth after centrifugation, so it will be used as raw materials for NR latex products. For sheets, it is produced from NR latex as ribbed sheets, by coagulation with acids and sheeting. For crepes, it is a type of crude natural rubber in the form of colourless or pale yellow crinkled sheets, prepared by pressing bleached coagulated latex through corrugated rollers. For block rubber, it is prepared by the following steps Firstly, filter NR latex in latex gathering tank, dissolve it to 20-25 % DRC and use 0.6 % of formic acid of weight to latex's rubber weight for coagulation. Then, roll the coagulated latex with crepe machine for 3 times, then the shredder machine. Next, heat the shredded rubbers for 4 hours at 100-110 °C, then compress in block of 33.33 kgs or 35 kgs with hydraulic machine. Finally, wrap with polyethylene bags and pack in cases. After production process finishes, a sample rubber has to be cut out for qualifications test and assess by statistic calculation before giving out quality certification to that series of rubber. For NR grade STR-5L, it is a Standard Thai Block Rubber that is a light colour rubber, processing from quality latex and converting rubber into crumbs and drying rubber at higher temperature of 100 °C. The uniform packing is 33.33 kgs in pressed bale as shown in Figure 2.4.
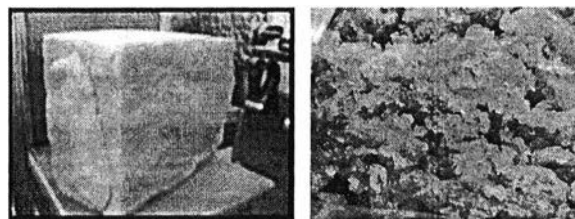
Figure 2.4 Block rubber grade STR 5L (left hand side) and masticated NR (right hand side).

Natural rubber is a linear polymer with the average molecular weight in range from 200,000 to 400,000 and with a relatively broad molecular weight distribution. This corresponds to about 3000 to 5000 isoprene units per polymer chain. As a result of its broad molecular weight distribution, NR has an excellent processing behavior. For other properties, NR is an amorphous material with low glass transition temperature (T_g) of -70 °C and specific gravity at 20 °C of 0.93. For this reason, NR is widely used as an impact modifier because its molecules can move under applied force to dissipate energy. Besides, it possesses many versatile properties; for example, low compression set, low hysteresis, low heat build-up, high resilience, and excellent fatigue resistance (Teh *et al.*, 2004; Mai and Yu, 2006). NR also has high elasticity, superior tensile strength and high tear resistance due to its long chain structure. The neat NR demonstrates a typical strain-induced crystallization behavior; that is, at lower strain region, the modulus is low and increases slowly with the increase of strain, but after approaching a certain value, the stress will rise sharply within a small range of strain due to the appearance and rapid development of tensile crystallization. From the rheological behavior point of view, pure NR displays the pseudoplastic behavior (viscosity decreases with increasing the shear rate) at lower shear rates, whereas at higher shear rates, it in turn shows the Newtonian behavior (viscosity becomes independent of the shear rate) (Stephen *et al.*, 2007). Thus, the commercial applications of NR are in the production of surgical gloves, balloons, tires, bumpers, etc. However, NR has limited ozone resistance and high dependence of dynamic properties on temperature (Arroyo *et al.*, 2007) and is known as an insulating material.

2.1.3 Polystyrene

Polystyrene (PS) is produced by the free radical polymerization of the styrene monomer, which is a derivative of petroleum. The chemical structure of PS shown in Figure 2.5 reveals that PS is composed of carbon and hydrogen atom only. Hence, it is classified as a hydrocarbon.
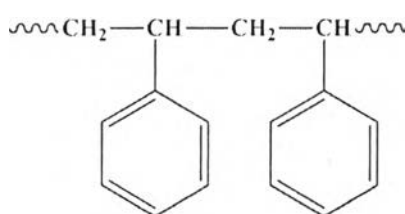

Figure 2.5 The chemical structure of polystyrene.

The presence of the pendant phenyl (C_6H_5) groups is a key to the properties of polystyrene. Solid PS is transparent, owing to these large, ring-shaped molecular groups, which prevent the polymer chains from packing into close, crystalline arrangements. In addition, the phenyl rings restrict rotation of the chains around the carbon-carbon bonds, lending the polymer its noted rigidity. PS is also a very inexpensive resin per unit weight. Unfilled PS has a sparkle appearance and is often referred to as crystal PS or general purpose polystyrene (GPPS). GPPS is clear, hard and brittle. It is also a rather poor barrier to oxygen and water vapor and has a relatively low melting point. Furthermore, as a thermoplastic polymer, PS is in a solid (glassy) state at room temperature but flows if heated above about 100 °C, its glass transition temperature (T_g). It becomes rigid again when cooled. This temperature behavior is exploited for extrusion, and also for molding (injection and compression) and vacuum forming, since it can be cast into molds with fine detail. It is very slow to biodegrade and therefore a focus of controversy, since it is often abundant as a form of litter in the outdoor environment, particularly along shores and waterways especially in its foam form.

Polystyrene is one of the most widely used plastics, the scale of its production being several billion kilograms per year. PS can be naturally transparent,

but can be colored with colorants. For packaging, food such as egg, meat, fish, poultry, and cold drinks or carry-out meals are safely packed with polystyrene packaging materials; by doing so spoilage of foods is prevented. PS is used for housing for TV's and all kind of emerging trends in IT equipment where the criteria for use are combinations of function, form and aesthetics and a high performance per cost ratio. PS is the leading choice for media enclosures, cassette tape housing and clear jewel boxes to protect CD's and DVD's. Due to its excellent price performance balance, good processability and other performance properties, PS resin is also among the most popular materials for building and construction applications, like insulation foam, roofing, siding, panels, bath and shower units, lighting, plumbing fixtures.

2.1.4 Dicumyl Peroxide

Dicumyl peroxide (DCP) is a white granular solid that melts at relatively low temperature (39 °C) and is essentially non-volatile at processing conditions. Hence, it is widely used as a high temperature catalyst in the rubber and plastics industries. DCP is an organic peroxide that its molecule contains two oxygen atoms connected by a single bond to organic chemical groups as shown in Figure 2.6. The chemical structure of DCP provides for near 100 % efficiency: all of the active oxygen contributes to reaction. In other words, this oxygen-oxygen bond is designed to break on heating, leaving one unpaired electron on each oxygen atom, called a "*free radical*". These free radicals are able to promote certain chemical reactions such as polymerization of one or more monomers for plastics manufacture, curing of thermosetting resins (polymer + monomer), crosslinking of elastomers, and grafting for polymer modification.
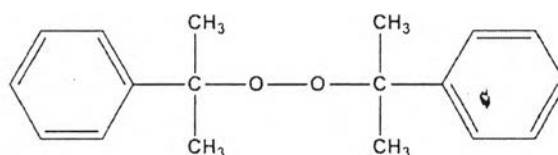

Figure 2.6 Dicumyl peroxide (DCP).

Generally, organic peroxides that are thermally decomposed generate free radicals; consequently, create an active site on a polymer backbone. The reaction between two active sites creates a strong link between the polymer chains, forming a polymer network and/or a graft copolymer that exhibits very desirable mechanical properties, particularly excellent heat resistance and compression set. Another advantage of using a peroxide initiator is the wide range of polymers that can be grafted and/or crosslinked (unsaturated polymers as well as saturated polymers like polyethylene). Tables 2.2 and 2.3 list the polymers that can and cannot be grafted and/or crosslinked by organic peroxides, respectively.

Table 2.2 Polymers crosslinkable with organic peroxides

Polymers	
Bromobutyl Rubber	BIIR
Polybutadiene Rubber	BR
Chlorinated Polyethylene	CM
Polychloroprene Rubber (Neoprene)	CR
Chlorosulfonyl Polyethylene	CSM
Ethylene Butylacrylate Copolymer	EBA
Ethylene Ethyl Acrylate	EEB
Ethylene Propylene Copolymer	EPM
Ethylene Propylene Diene Terpolymer	EPDM
Ethylene Vinylacetate Copolymer	EVA
Hydrogenated Acrylonitrile-butadiene Rubber	HNBR
Polyisoprene Rubber	IR
Acrylonitrile-butadiene Rubber (Nitrile Rubber)	NBR
Natural Rubber	NR
Polyethylene (includes high, low and linear low density)	PE
Styrene-butadiene Rubber	SBR

Table 2.3 Polymers not crosslinkable with organic peroxides

Polymers	
Polyacrylate Rubber	ACM
Chlorobutyl Rubber	CIIR
Butyl Rubber	IIR
Polybutene	PB
Polyisobutylene	PIB
Polypropylene	PP
Polyvinylchloride	PVC

As mentioned above, DCP decomposes when heated to form alkoxy radicals that, in turn, abstract hydrogen from the polymer backbone, forming polymer radicals. A combination of two polymer radicals results in graft copolymer and/or polymer network. In general, the rate of crosslinking is equivalent to the rate of DCP thermal decomposition that is dependent primarily on processing temperature and is predictable for each polymer system.

"*Half-Life*" is a term that is used to describe peroxide crosslinking reactions. The half-life is the time it takes one-half of any quantity of peroxide present to thermally decompose. This time is primarily dependent on temperature but is independent of the quantity of peroxide present. In the first half-life, 50 % of the peroxide decomposes. During the second half-life, 50 % of the remaining peroxide decomposes. This is 25 % of the original quantity, and the total amount decomposed is now 75 %. The process continues and theoretically never reaches 100 % decomposed. Practically, the level is so low after seven half-lives that the effect of additional cure time is insignificant. Table 2.4 shows the relationship between number of half-life and the portion of the peroxide that has been decomposed.

Table 2.4 Relationship between half-life and decomposition of DCP

Half-Life	Amount of Original Decomposed Peroxide (%)
1	50.00
2	75.00
3	87.50
4	93.75
5	96.90
6	98.40
7	99.20
8	99.60
9	99.80
10	99.90

Figure 2.7 is a plot of the crosslinking half-life of DCP in various systems. In addition to the polymers shown, cis-polybutadiene (BR) has a half-life curve between those of nitrile rubber (NBR) and ethylene-propylene terpolymer (EPDM). Polyisoprene (IR), natural rubber (NR), and styrene-butadiene rubber (SBR) have approximately the same half-life curves, and this common curve lies between those of NBR and the solution.
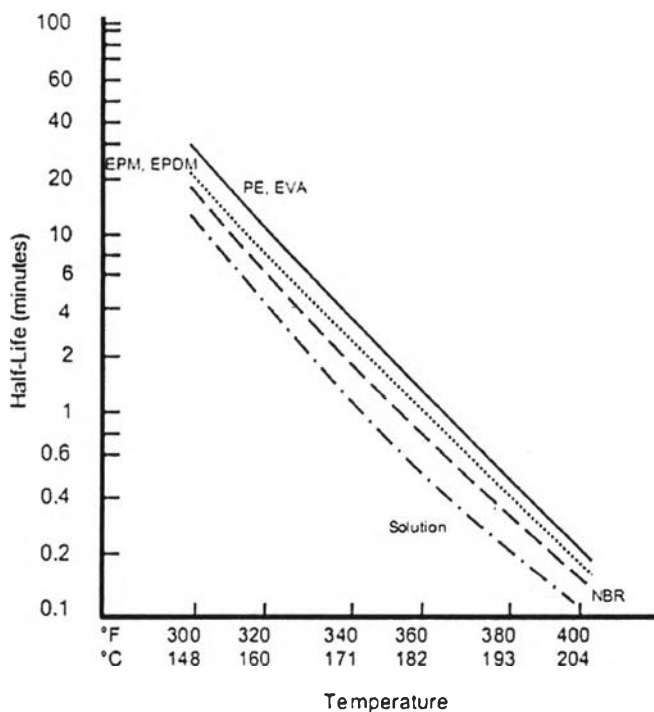
Figure 2.7 Half-Life of dicumyl peroxide (DCP) *versus* Temperature in Various Polymers (Reprinted from Technical information of Arkema Inc).

From these results, the half-life time of DCP in natural rubber (NR) system at processing temperature of 170 °C is 1.65 min approximately. The efficiency of crosslinking is primarily dependent on the amount of decomposed peroxide (%). The higher amount of decomposed peroxide, the higher content of crosslinked NR (gel) is obtained. The percentage (%) of peroxide decomposed can be calculated by using Equation (2.1).

$$\text{Percent of peroxide decomposed} = (1 - 0.5^N) \times 100 \qquad (2.1)$$

where N is the number of peroxide half-life. In this research work, a graft copolymer of polystyrene and natural rubber (PS/NR) was prepared in twin-screw extruder (Labtech) with a screw diameter of 20 mm and a length/diameter ratio of 44. Dicumyl peroxide (DCP) was added into the system to be an initiator at processing temperature of 170 °C with various screw speeds (30-45 rpm). The content of

crosslinked NR or gel related to the amount of peroxide decomposed was then investigated. Table 2.5 shows the correlation of resident time at different screw speeds and amount of decomposed peroxide (%) of PS/NR blend. The result shows that high screw speed provides short resident time on extrusion, resulting in less amount of peroxide decomposed. It leads to the lowering of gel (crosslinked NR) content in the PS/NR blend using high screw speed of 45 rpm which the result will be discussed in Chapter IV.

Table 2.5 Resident time at different screw speeds *versus* amount of decomposed peroxide (%) of PS/NR blend prepared in twin-screw extruder at processing temperature of 170 °C

Screw Speed (rpm)	Resident Time (min)	No. of Half-life (Half-life Time = 1.6 min at 170 °C)	Amount of Decomposed Peroxide (%)
30	7.5	4.5	95.58
35	6.0	3.6	91.75
40	4.5	2.7	84.61
45	3.0	1.8	71.28

2.2 Rubber-toughened Plastics

The development of rubber-toughened thermoplastic resins is an important contribution to the commercial polymer industry. The aim of toughening is mainly to increase the impact strength beyond a given target with a tolerated loss in stiffness (modulus), yield stress and creep resistance. Generally, a small amount of discrete rubber particles in the plastic can greatly improve the crack and impact resistance of amorphous polymers such as polystyrene (PS), polycarbonate (PC) and polyvinylchloride (PVC), and of semicrystalline polymers including polyamides

(PA), polypropylene (PP), and thermoplastic polyesters such as polyethylene terephthalate (PET) and polybutylene terephthalate (PBT).

Rubber toughening is a technique of incorporation of 10-25 % rubber into rigid thermoplastics in order to increase the toughness. When the toughened materials are strained, crazes will form at their surfaces, resulting in the increasing of energy needed to break the material. For polymer/rubber blend system, Bucknall (1977) and Keskkula (1989) stated that the toughness of polymers is improved by the dispersion of rubber particles, and the toughening mechanism can be explained by the plastic deformation (crazing, shear yielding, etc.) of the polymer matrix around these rubber particles and the cavitation of rubber particles.

Crazing and shear yielding are the two primary localized deformation mechanisms of polymers. Crazing occurs when localized regions yield, forming an interconnected array of microvoids. Fibrillar bridges of oriented molecular chains form between voids. At high enough tensile loads, these bridges elongate and break, enabling crack propagation as shown in Figure 2.8. Crazing absorbs fracture energy and increases fracture toughness. Generally, crazes are initiated in glassy thermoplastics (PS and SAN) if the local tensile stress exceeds some specific value.

Fibrillar bridges   Microvoids   Crack

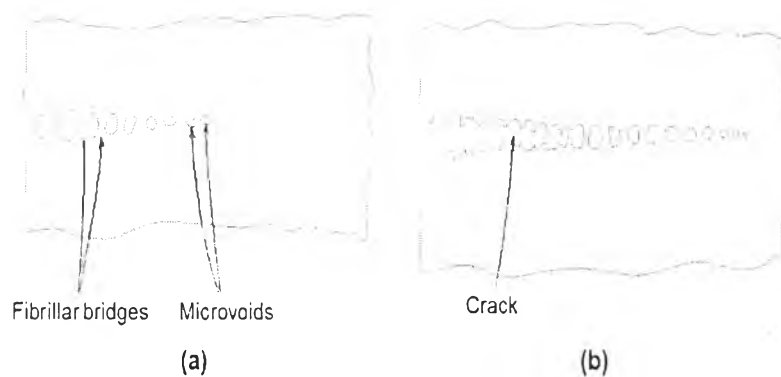(a)   (b)

Figure 2.8 Schematic drawings of (a) a craze showing microvoids and fibrillar bridges, and (b) a craze followed by a crack (Reprinted from Callister and Rethwisch, 2010).

Shear yielding is the process by which ductile polymer materials extend to high strain in standard test. The chain segments slip past each other in response to shear test, with the result that a small element of the materials in the yield zone changes shape while remaining close to constant volume. Upon further deformation, the material hardens due to molecular orientation and this leads to multiplication and propagation of shear bands as shown in Figure 2.9. Shear yielding is thought to precede ductile failure because fracture involves relatively large deformations, resulting from relatively high energy dissipation. In addition, the shear yielding mechanism is better suited to a lower particle size than the crazing mechanism.
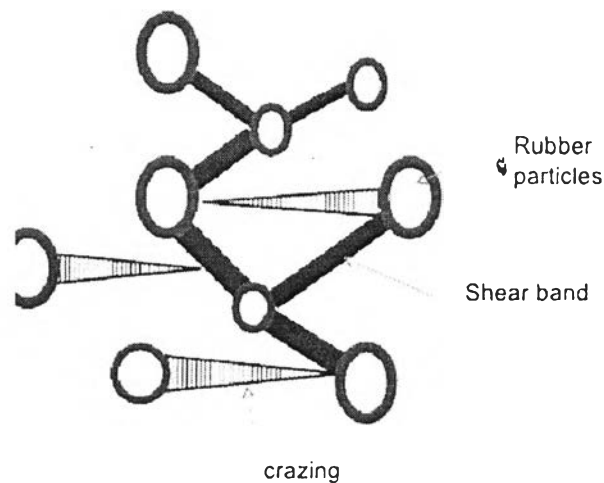

Figure 2.9 Plastic deformation by crazing and shear yielding (Reprinted from Shahid, 2010).

The cavitation in rubber particles plays an important role in the toughening mechanism as seen by stress whitening region in many rubber-modified plastics systems. However, the particle size of rubber phase strongly affects to its cavitation. The rubber particle size over 5 μm is often too large to interact with the stress field at the crack tip while rubber particle size under 0.1 μm is too small to cavitate effectively (Walker and Collyer, 1994).

Correa and Sousa (1997) studied the cavitation process of high impact polystyrene (HIPS) from tensile and impact specimens. Under stress (applied load), the result showed the cavitation of rubber particles, and then it accelerated the crazing in the PS matrix as shown in Figure 2.10.
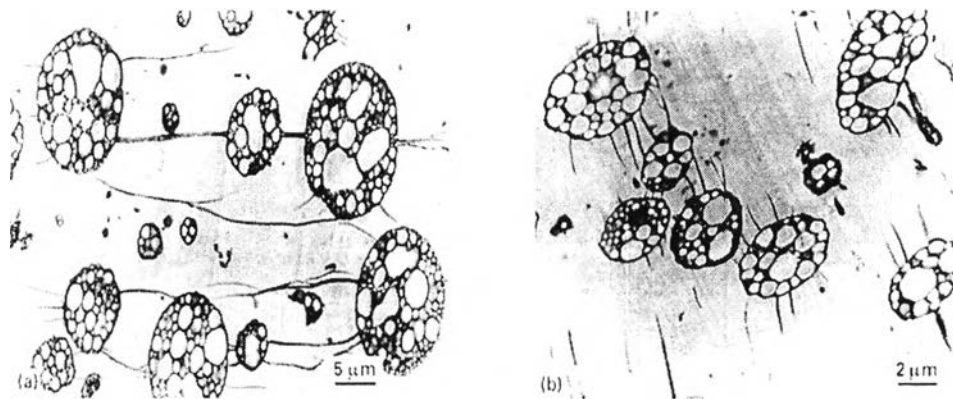
Figure 2.10 TEM micrographs show the evidence of rubber cavitation and crazing initiation in HIPS blends; (a) tensile specimen; (b) notch region of impact specimen.

In rubber-toughened polyamide systems, Majumdar *et al.* (1994) stated that the rubber cavitation was found in the deformed zone of the compatibilized Nylon6/ABS/IA (45/45/10) blends. The white region in Figure 2.11(A) and the black hole in Figure 2.11(B) were the rubber cavitation of butadiene particles. In addition, the rubber cavitation would be occurred in the rubber particles having size larger than 0.2 µm.
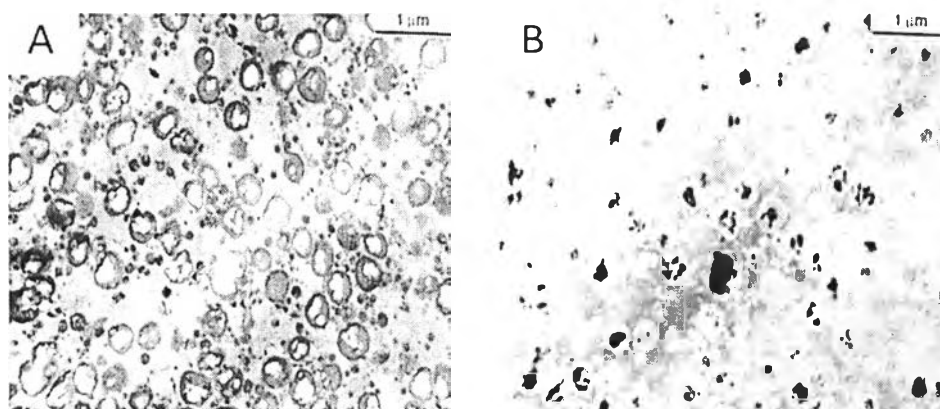

Figure 2.11 TEM photomicrographs from the deformed zone of the compatibilized Nylon6/ABS/IA (45/45/10) blend taken at the following locations: (A) far away from the crack tip (~ 2 mm) and (B) same as in (A) but under dark field.

2.3 Polymer Blend

Two or more existing polymers may be blended for various reasons. One reason is to achieve a material that has a combination of the properties of the constituents, e.g. a blend of two polymers, one of which is chemically resistant and the other tough. Another reason is to save costs by blending a high-performance polymer with a cheaper material. A very important use of blending is the combination of an elastomer with a rigid polymer in order to reduce the brittleness of the rigid polymer.

2.3.1 Method of Polymer Blending

The blending process allows the intensive transfer of polymer chains that occurs at the polymer-polymer interfaces to obtain a homogeneous blend. The homogeneity of polymer blend depends on the nature of the blend components and the blending techniques.

2.3.1.1 Polymerization

This method is mainly about an emulsion polymerization. The polymers are required to be latex or emulsion form. The mixing process of these microsize latexes and the subsequent removal of water produce excellent dispersion and distribution of discrete phase.

2.3.1.2 Solution casting

The requirement of this method is that the polymers need to be dissolved in a common solvent. The blend is produced by evaporating the solvent and precipitating the resulting polymer mixture. Good molecular level of mixing can be achieved with cost depending on the solvent and its recovery.

2.3.1.3 Mechanical Blending

The blend properties are strongly influenced by the speed and temperature of mixing which the homogeneous blend is only obtained after the melt processing state. High-shear mixers can generate fine dispersions, with droplet diameters less than 1 μm.

2.3.1.4 Reactive Blending

The process usually involves an addition of a third reactive component, i.e., a multifunctional copolymer or trans-reactive catalyst. Improved compatibility of reactive blends is usually due to the emulsifying effects of interchain block or graft copolymers that are formed during melt mixing. This method provides more homogeneous blending with high productivity.

2.3.2 Miscibility of Polymer Blend

For the properties of polymer blends, not only the productions (polymerization, solution casting, melt mixing, and reactive blending) but also the miscibility of polymer blends has played an important role in the improvement of their properties. In general, polymer blend can be divided into two major classes based on their thermodynamic phase behavior.

2.3.2.1 Miscible Polymer Blend

It is well known that due to thermodynamic limitations, only a few polymers form truly miscible blend, characterized by a single T_g and homogeneity at the molecule level. When two polymers, A and B form a homogeneous mixture, many properties of the blend are additive (Olabisi et al., 1979; Paul and Barlow, 1980). A thermodynamic condition for miscibility involves an appropriate balance of the enthalpy and entropy terms in the Gibbs free energy of mixing, i.e., the free energy of mixing ΔG_{mix}, must be negative as described in Equations (2.2)-(2.4).

$$\Delta G_{mix} = \Delta H_{mix} - T\Delta S_{mix} \tag{2.2}$$

If $\quad \Delta G_{mix} < 0,$ (2.3)

Then $\quad \Delta H_{mix} - T\Delta S_{mix} < 0,$ (2.4)

where ΔH_{mix} is the enthalpy of mixing (heat of mixing), ΔS_{mix} is the entropy of mixing with T being the temperature. Equation (2.4) implies that exothermic mixture ($\Delta H_{mix} < 0$) and a thermal mixture ($\Delta H_{mix} = 0$) will mix spontaneously, whereas for

endothermic mixture ($\Delta H_{mix} > 0$) miscibility will only occur at high temperature (Bonner and Hope, 1993).

Thus for the miscible polymer blend, the favorable entropic contribution must be large enough to yield a negative free energy of mixing. For the enthalpic part, negative, zero or small positive ΔH_{mix} values are required for miscibility.

2.3.2.2 Immiscible Polymer Blend

Most polymer blends are immiscible due to their small combinatorial entropy of mixing and their positive enthalpy of mixing when specific interactions between components are absent. The thermodynamic condition for immiscible blend also involves a balance of the enthalpy and entropy terms in the Gibbs free energy of mixing as shown in Equation (2.2) but the free energy ΔG_{mix} will be positive as seen in Equation (2.5) (Olabisi *et al.*, 1979). Hence, phase separation can occur.

$$\Delta G_{mix} > 0, \qquad (2.5)$$

$$\text{if} \qquad \Delta H_{mix} > 0 \qquad (2.6)$$

For low molecular weight materials, the increasing of miscibility can be done by increasing temperature. As a consequence, the increasing of $T\Delta S_{mix}$ term drives ΔG_{mix} to more negative values. For high molecular weight polymer blends, the gain in entropy is negligible. Hence, the free energy of mixing can only be negative if the heat of mixing (enthalpy of mixing) is negative. This means that the mixing must be exothermic, which usually requires specific interactions between the blend components. These interactions may range from strongly ionic to weak and non-bonding, including hydrogen bonding, ion-dipole, dipole-dipole, and donor-acceptor interactions. However, most polymer blends show the positive values of ΔH_{mix} as seen in Equation (2.6) due to the lack of these specific interactions causing phase separation on blending.

The other basic theory for assessing the miscibility of polymer blends was developed by Flory (1941, 1942); Huggins (1941, 1942) and is thus referred to as the Flory-Huggins theory. The Equation (2.7) resulting from their analysis is termed the Flory-Huggins Equation as noted:

$$\Delta G_{mix} = kTV\left[\frac{\varphi_1}{V_1}\ln\varphi_1 + \frac{\varphi_2}{V_2}\ln\varphi_2\right] + \varphi_1\varphi_2\chi_{12}kTV/\upsilon_r \qquad (2.7)$$

where V is the total volume, V_i is the molecular·volume of component i, ϕ_i is the volume fraction of component i, k is the Boltzmann's constant, χ_{12} is the Flory-Huggins interaction parameter and υ_r is the interacting segment volume (such as a repeat unit volume) and is also referred to as the reference volume. This equation was primarily employed for solvent-polymer mixtures but is applicable to higher molecular weight polymer mixtures. The Flory-Huggins Equation was successfully applied to demonstrate the basic reason for decreased miscibility of solvent-polymer mixtures compared to solvent-solvent mixtures as the combinatorial entropy of mixing is decreased. With polymer-polymer mixtures, the combinatorial entropy of mixing (the bracketed terms) approaches insignificant values in the limit of high molecular weight polymer mixtures. Thus the Gibbs free energy of mixing only depends on the heat of mixing (the second term on the right-hand side). It also relates to the Flory-Huggins interaction parameter as shown in Equation (2.8). To achieve miscibility, a negative heat of mixing must be obtained (i.e., $\chi_{12} < 0$).

$$\Delta H_{mix} = \varphi_1\varphi_2\chi_{12}kTV/\upsilon_r \qquad (2.8)$$

The solubility parameter can be used for a predictive capability of assessing the potential of miscibility of materials. The concept was reported by Hildebrand (1916) where the solubility of a material was noted to be influenced by the solvent internal pressure. This concept was further developed by Scatchard (1931). Scatchard defined the cohesive energy density (CED) as the energy of vaporization (E_v) per unit volume (V). Hildebrand (1936) then defined the

solubility parameter (δ_p) as the square root function of the cohesive energy density seen in Equation (2.9).

$$\delta_p = (CED)^{1/2} = \left(\frac{\Delta E_v}{V}\right)^{1/2} \tag{2.9}$$

The basic concept involves matching the solubility parameter to achieve miscibility. For solvent-solvent mixtures, the difference of solubility parameter is very significant for miscibility to be achieved. With solvent-polymer mixtures, the solubility parameter difference is still significant and works well for non-polar solvent mixtures with some divergence for highly polar or hydrogen bonding liquids as well as other specifically interacting molecules. For polymer-polymer mixtures, the solubility parameters need to be virtually identical to achieve miscibility in the absence of strong polar or hydrogen bonding interactions. However, the energy of vaporization of polymers cannot be determined. Therefore, the solubility parameter of polymers is typically determined by swelling a crosslinked sample in a series of solvents and assigning the solubility parameter value where the highest swelling (best solvent) occurs. Although the solubility parameter approach has some qualitative utility, the inability to address specific interactions is a major limitation. Equation (2.10) shows the relationship of Flory-Huggins interaction parameter with the solubility parameter.

$$\frac{\chi_{12}}{\upsilon_r} = (\delta_{p1} - \delta_{p2})^2 / RT \tag{2.10}$$

and thus negative values (indicative of specific interactions) cannot be obtained.

The immiscible mixture of polymers shows multiple amorphous phases as determined, for instance, by presentation of multiple glass transition temperatures. Blends of immiscible polymer have complex properties that are rarely additive (Olabisi et al., 1979; Paul and Barlow, 1980). The poor

mechanical behavior of phase separation blends is usually the consequence of inadequate adhesion between phases that does not allow efficient transfer for stress across the interface. However, the immiscible blend is called compatible if it is a useful blend which the inhomogeneity caused by the different phases is on a small enough scale not to be apparent in use. In other words, blends that are miscible in certain useful ranges of composition and temperature, but immiscible in others, are also sometimes called compatible blends. Most immiscible polymer blends can be made compatible only by a variety of compatibilization techniques. Such compatibilized blends are sometimes called polymer alloys.

2.4 Compatibilization

Compatibility is frequently defined as miscibility on a molecular scale (Krause, 1978). Another way of defining compatible blends is as polymer mixtures which do not exhibit gross symptoms of phase separation on blending. A third definition is to consider blends as compatible when they possess a (preferably commercially) desirable set of properties.

2.4.1 Compatibilization Mechanisms

For immiscible polymer blend, melt mixing of two polymers results in blends which are weak and brittle. Since the incorporation of a dispersed phase in a matrix leads to the presence of stress concentrations and weak interfaces, arising from poor mechanical coupling between phases. In general, the mechanical properties of the blend will be determined not only by the properties of its components but also by the phase morphology and the interfacial adhesion. These factors are important from the viewpoint of stress transfer within the blends in their end-use applications. Furthermore, the factors affecting phase morphology such as the process (mixer type, rate of mixing and temperature history), the rheology of the blend components, and the interfacial tension between phases in the melt are also important (see Figure 2.12). To improve the total blend performance, the immiscible blends usually need compatibilization.

Compatibilization is any physical or chemical process of modification of interfacial properties in the immiscible polymer blend. One aim of compatibilization is to reduce the interfacial tension in the melt, causing an emulsifying effect and leading to an extremely fine dispersion of one phase in another. Another aim is to increase the adhesion at phase boundaries, giving improved stress transfer. A third aim is to stabilize the desired morphology, leading to the creation of a polymer alloy.
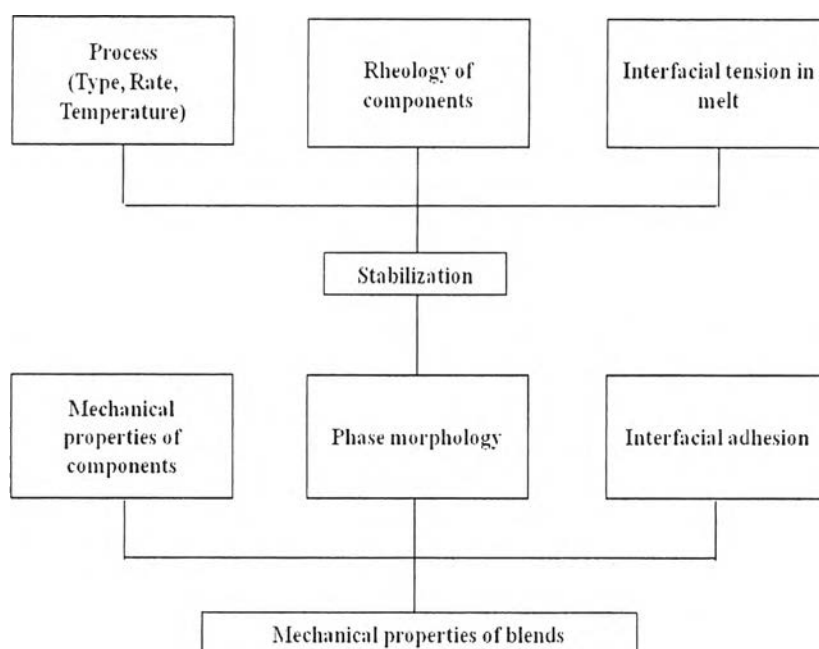

Figure 2.12 Summary of the factors contributing to the end-use properties in melt compounded blends (Redrawn from Bonner and Hope, 1993).

2.4.2 <u>Compatibilization Methods</u>

For modification of blends to produce a desired set of properties, a number of different methods of compatibilization would be defined.

2.4.2.1 Achievement of Thermodynamic Miscibility

As mentioned previously, miscibility between polymers is determined by a balance of enthalpic and entropic contributions to the free energy of mixing. For small molecules, the entropy is high enough to ensure miscibility. For

high molecular weight polymers, the entropy is almost zero, causing enthalpy to be decisive in the determining miscibility. The change in the Gibbs free energy of mixing (ΔG_{mix}) is shown in Equation (2.2). For spontaneous mixing, ΔG_{mix} must be negative. Hence, the exothermic mixtures ($\Delta H_{mix} < 0$) will mix spontaneously whereas for the endothermic mixtures miscibility will occur at high temperatures. The phase diagrams exhibiting upper or lower critical solution temperature (UCST or LCST) for two-component blends are shown in Figure 2.13. UCST is the critical temperature above which the components of a mixture are miscible in all proportions, and the phase separation occurs when temperature decreases. LCST behavior is more commonly seen. Mixing of the two phases is spontaneous below the LCST, and phase separation occurs as temperature increases. Since the intermolecular attractive forces responsible for the miscible behavior tend to disappear as the internal energy of the molecules become high enough to overcome them. Hence, it is possible to tailor the structure of polymers in some circumstances to modify their phase diagram in blends, and thereby to achieve miscible blends.
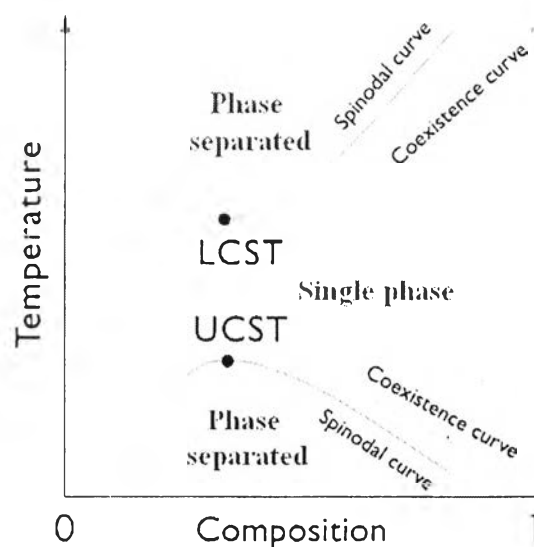

Figure 2.13 Schematic phase diagrams for binary blend exhibiting UCST and LCST behavior (Reprinted from Cowie and Arrighi, 2008).

2.4.2.2 Addition of Block and Graft Copolymers

Block and graft copolymers containing segments chemically identical to the blend components are used as compatibilizers. These copolymers locate preferentially at the blend interfaces as shown in Figure 2.14. The miscibility between the copolymer segments and the corresponding blend components is assured, providing the copolymer meets certain structural and molecular weight requirements.
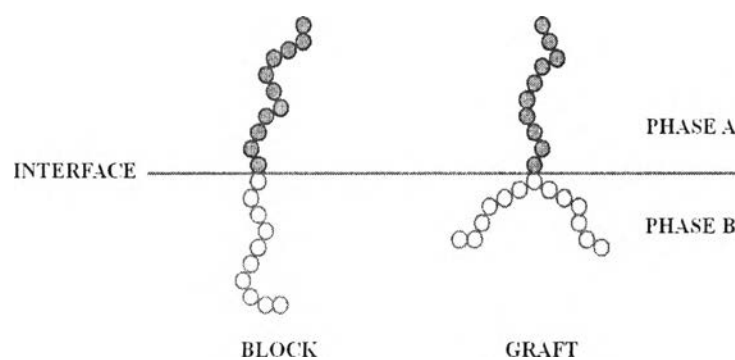

Figure 2.14 Schematic diagram showing location of block and graft copolymers at interface (Redrawn from Bonner and Hope, 1993).

Structure and molecular weight of block and graft copolymers have important influences on their effectiveness as compatibilizers. Fayt *et al.* (1981a, 1981b, 1982, 1989) studied the effect of different copolymer types on the compatibility of PE/PS blends. They concluded that block copolymers were more effective than graft copolymers. In addition, diblock copolymers were more effective triblock copolymers, and tapered diblock copolymers were more effective than pure diblock copolymers. For molecular weight, the solubilization of a dispersed homopolymer into its corresponding domain of block copolymer used as compatibilizer only occur when the homopolymer molecular weight is equal to or less than that of the corresponding block. However, stabilization of a matrix homopolymer into its corresponding domain of block copolymer will occur even if the molecular weights are mismatched (Paul, 1978). Hence, the balanced molecular weight is needed for copolymer compatibilizer; the segments need to be long enough

to anchor to the homopolymer (i.e. to stabilize) but short enough to minimize the amount of compatibilizer needed for cost-effective processing.

2.4.2.3   Addition of Functional Polymers

In general, a polymer chemically identical to one of the blend components is modified via a reactor or an extrusion-modification process to contain functional or reactive units which have some affinity for the second blend component. The functionalized blend component has the ability to chemically react with the second blend component, but other types of interaction (e.g. ionic) are possible. For instance, grafting of maleic anhydride or similar compound to polyolefins provides the pendant carboxyl groups having the ability to form a chemical linkage with polyamide via their terminal amino groups. Besides, the polymers functionalized with maleic anhydride or acrylic acid are commercially available at acceptable cost to be used as compatibilizers.

2.4.2.4   Reactive Blending

Reactive blending is the *in situ* formation of copolymers or interacting polymers (Bonner and Hope, 1993). The blend components themselves are either chosen or modified so that reaction occurs during melt blending, with no need for addition of a separate compatibilizer. A number of reactive blending mechanisms may be exploited:

- Formation *in situ* of a block or graft copolymer by chemical bonding reaction between reactive groups on the blend components. This reaction may be stimulated by addition of a free radical initiator during mixing.

- Formation of a block copolymer by an interchange reaction in the backbone bonds of the condensation polymers.

- Mechanical scission and recombination of the blend components to form graft or block copolymers during high shear level mixing.

- Promotion of reaction by catalysis.

Considering the above mentioned, there is clearly overlap between these approaches. Hence, the use of these methods depends on the requirements of the situation such as the properties of materials, the facilitation of blend processing and economic factors.

2.4.3 Roles of Compatibilizer

Generally, there are three main roles of a compatibilizer in the blending process. Firstly, it decreases the interfacial tension between the blend components and so retards the formation of the Rayleigh disturbances on the generated threads of dispersed phase. The lower the interfacial tension, the longer the deformation tension exceeds the interfacial tension, the longer the stretching of the thread proceeds, the smaller the diameter of the resulting thread becomes, and, consequently, the finer the size and dispersion of the generated dispersed phase. Secondly, the compatibilizer improves the interfacial adhesion in the solid state. This can be obtained either by ascertaining that an appropriate concentration of covalent bonds crosses the interface, by adding a compatibilizer that can act as an adhesive between two components, and/or by controlling the morphology, especially by inducing the phase co-continuity. The enhanced adhesion facilitates efficient stress transfer from one phase to the other phase and prevents cracks initiated at the interface from growth until the occurrence of catastrophic failure. Finally, block or graft copolymers used as compatibilizers inhibit the coalescence process of the dispersed phase via steric stabilization during subsequent blending. These compatibilizers can prevent coalescence both dynamic (flow-driven) coalescence and static coalescence resulting in phase size reduction and morphology stability or compatibilization, respectively. Figure 2.15 illustrates the effect of a compatibilizer on the blend morphology development. If enough block or graft copolymers can diffuse to the freshly generated interface, it should reduce the interfacial tension, permitting sheets to be drawn down thinner and prevent drop coalescence. Macosko *et al.* (1996) estimated that less than 5 % of the interface needs to be covered to prevent dynamic coalescence, while about 20 % is necessary to impart static stability. However, a dramatic reduction in the coalescence rate has been reported when a small amount of compatibilizer is added to polymer blends. Due to the fact that the droplet size decreases with compatibilizer, the number of droplets per volume unit increases and the separation distance between droplets decreases at a constant volume fraction of the dispersed phase. This results in an increase of flow-driven coalescence (Huitric *et al.*, 2007).
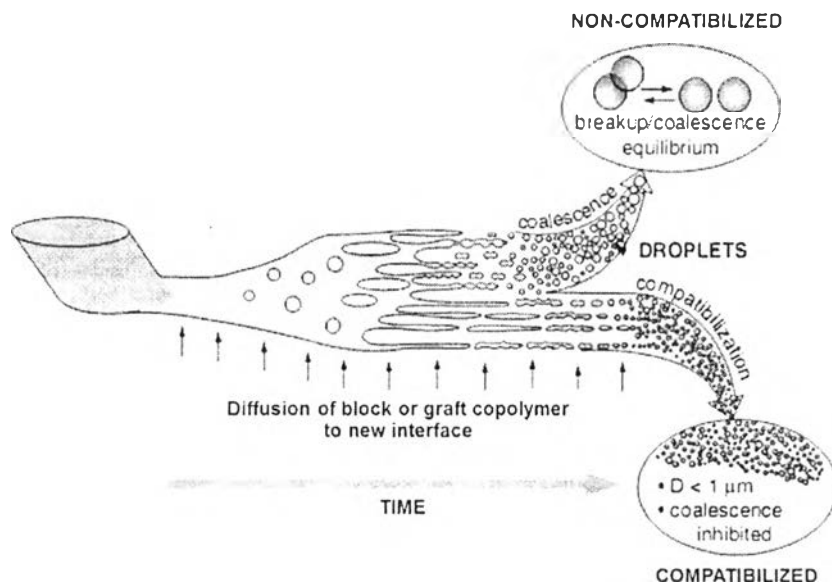
Figure 2.15 Schematic of morphology development during melt blending without and with a compatibilizer (Reprinted from Macosko *et al.*, 1996).

For coalescence of particle, it is a process that two or more particles collide and physically merge into one particle. As mentioned previously, two classes of coalescence play critical roles in the development of morphology during the processing of immiscible polymer blends. The *flow-driven or dynamic coalescence* is a growth process that single particles grow together during shearing as shown in Figure 2.16. A small particle (A) moves towards a large particle (E) following a streamline and coalesces with it (B) or passes by, but does not coalescence (C). Particles can deform when they approach to each other as seen by (D). Due to their motion along streamlines, only those particles within the region of y_c coalesce with the large one. Otherwise, all the particles in the region of $D_A + D_E$ would coalesce (where D_A and D_E are the particle diameters). The arrows inside the drops show the fountain flow. During flow, a steady-state balance between the flow-driven coalescence and breakup produces a population of particles with a specific size distribution.
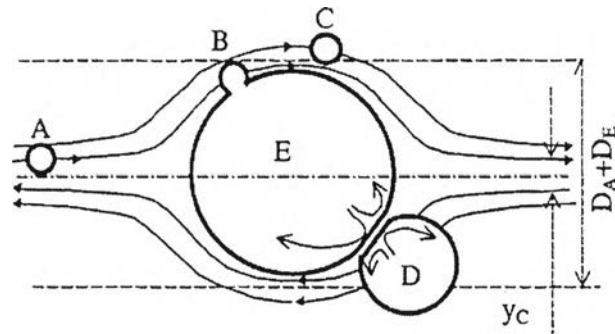
Figure 2.16 Particle-particle coalescence (Reprinted from Lyu *et al.*, 2000).

Annealing via an additional thermal treatment or an aging process or some mechanical energy supply leads to *static coalescence*, a mechanism that reduces interfacial area through particle-particle fusion. The driving forces for the static coalescence are complicated by such factors as Brownian motion, Van der Waals interactions, particle reshaping, and sedimentation. Hence, the flow-driven coalescence actually is simpler to model than the static coalescence, and it is more suitable for studying the general mechanism of coalescence than the conventional static coalescence (Lyu *et al.*, 2000).

2.5 Rheology

Rheology is a branch of physics that deals with the deformation and flow of material under stress. The rheology establishes not only the relationship between applied forces and geometrical effects induced by these forces, but also the relationship between rheological properties of material and its molecular structure (composition). This is related to estimating the quality of materials, understanding the laws of molecular movements and intermolecular interaction (Malkin and Isayev, 2006). For simple fluids, the rheological study involves the measurement of viscosity depending upon temperature and hydrostatic pressure. For polymer, due to its viscoelastic behavior, the viscosity of polymeric fluids depends on shear rate, molecular weight, polymer structure, concentration of various additives, and temperature.

2.5.1 <u>Measurement of Viscosity</u>

For shear flow, the material is confined between two plat plates of area A separated by a distance D. Then, a force F is applied to move the upper plate at a constant velocity relative to the lower plate as shown in Figure 2.17.
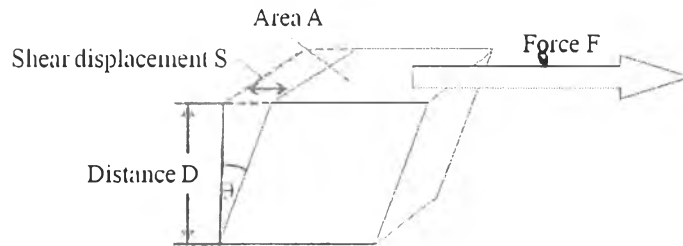
Area A

Shear displacement S

Force F

Distance D

Figure 2.17 Schematic diagram for the measurement of shear viscosity (Redrawn from Nielsen, 1977).

The force is directly proportional to the viscosity of material. The important quantities involved in measuring shear viscosity are defined as the following Equations (2.11)-(2.13);

$$\text{Shear stress } (\tau) = \frac{\text{Shear force (F)}}{\text{Area of shear face (A)}} \tag{2.11}$$

$$\text{Shear strain } (\gamma) = \frac{\text{Shear displacement (S)}}{\text{Distance between sheaaring surfaces (D)}} = \tan\theta \tag{2.12}$$

$$\text{Viscosity}(\eta) = \frac{\text{Shear stress } (\tau)}{\text{Shear strain rate}(\gamma)} \tag{2.13}$$

For Newtonian fluids (ideal fluids), the shear stress is proportional to the deformation rate (shear rate) as shown in Figure 2.18. Thus, their viscosity (slope of plot between shear stress and shear rate) is a constant and independent of shear rate.
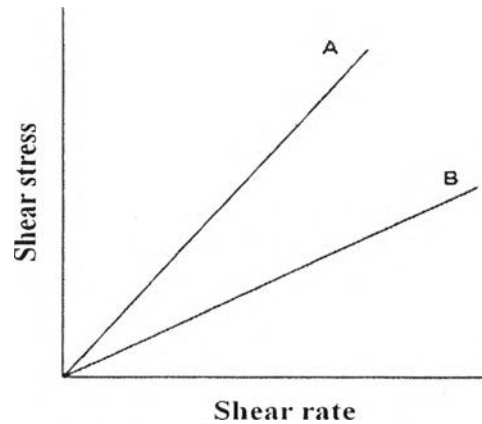
Figure 2.18 Rheogram of Newtonian liquids; A for high viscosity and B for low viscosity (Reprinted from Nielsen, 1977).

For non-Newtonian fluids, the shear stress is not proportional to the shear rate, in other words, the plot of shear stress against shear rate is not linear. The relationship between shear stress and shear rate or "flow curve" is generated according to the Ostwald-de Waele equation or "the power law equation" (Brydson, 1970) as shown in Equation (2.14) and Figure 2.19. Hence, the viscosity of non-Newtonian fluids also depends on shear rate as shown in Equation (2.15).

$$\tau = K(\dot{\gamma})^n \tag{2.14}$$

$$\eta = K(\dot{\gamma})^{n-1} \tag{2.15}$$

where τ is the apparent shear stress (Pa), η is the apparent shear viscosity, $\dot{\gamma}$ is the apparent shear rate (s^{-1}), K is the flow consistency index or the viscosity coefficient index, and n is the flow behavior index or the power law index.
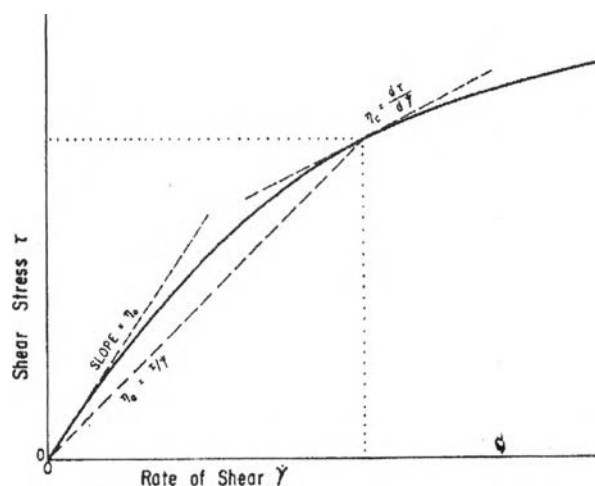
Figure 2.19 The relationship between shear stress and shear rate for non-Newtonian fluids (solid line) compared to Newtonian fluid (dash line) (Reprinted from Nielsen, 1977).

2.5.2 Capillary Rheometer

Capillary rheometer is the most effective instrument for qualitative estimation and viscosity measurement. This is due to the simplicity of experiment units, relative inexpensive, and ease to standardize test procedure. The essence of method is that the material is forced by a piston or by pressure from reservoir through a capillary (cylindrical tube with large length-to-radius, L/R) as shown in Figure 2.20.
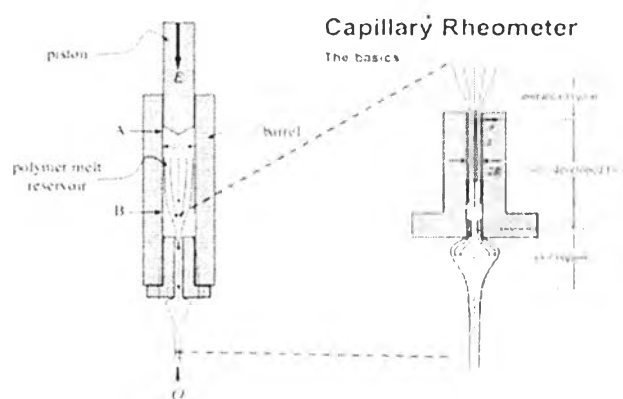

Figure 2.20 Schematic diagram of capillary rheometer (Reprinted from Morrison, 2014).

The quantity of polymer coming from the capillary per unit of time at a given pressure drop is the basic measurement used to calculate the viscosity. For Newtonian fluids, according to Hagen-Poiseuille law (Cogswell, 1996) the important parameters relating to the capillary rheometer are shown in Equation (2.16).

$$\tau_w = \frac{R\Delta P}{2L} \tag{2.16}$$

where τ_w is the shear stress at wall, R is the radius of the die (mm), ΔP is the pressure drop across the die (Pa), and L is the length of the die (mm); and the shear rate at wall (γ_w) is defined as shown in Equation (2.17).

$$\gamma_w = \frac{4Q}{\pi R^3} \tag{2.17}$$

where Q is the volumetric flow rate. Then, the viscosity (η) is calculated from the ratio of shear stress to shear rate as seen in Equation (2.18).

$$\eta = \frac{\tau_w}{\gamma_w} = \frac{\pi R^4 \Delta P}{8LQ} \tag{2.18}$$

For non-Newtonian fluids, two corrections are commonly applied to capillary data in order to obtain the correct viscosity of polymeric fluids. Unless a very long capillary is used (L/D>100), entrance pressure drop may considerably affect the accuracy of the measurements. Hence, the Bagley correction is used to correct the pressure drop from the entrance and exit effects (Brydson, 1970; Cogswell, 1996). For this correction, ΔP would be separated into ΔP_{ent} (entrance pressure drop), ΔP_{cap} (pressure drop inside capillary die) and ΔP_{ex} (exit pressure drop) as shown in Figure 2.21.
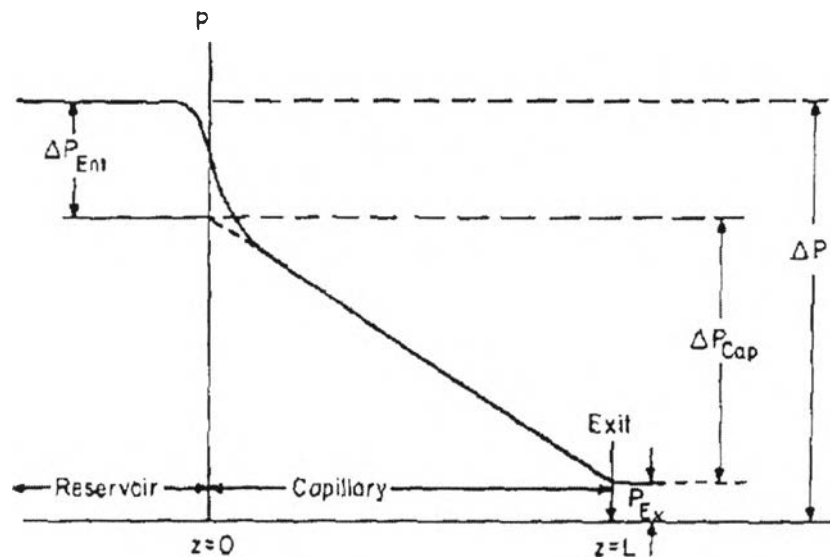
Figure 2.21 Pressure distribution in both the reservoir and the capillary (Reprinted from Brydson, 1970).

Three or four capillaries (different die length, L) are used. Then, the pressure drop in each shear rate is plotted as a function of L/R as shown in Figure 2.22.
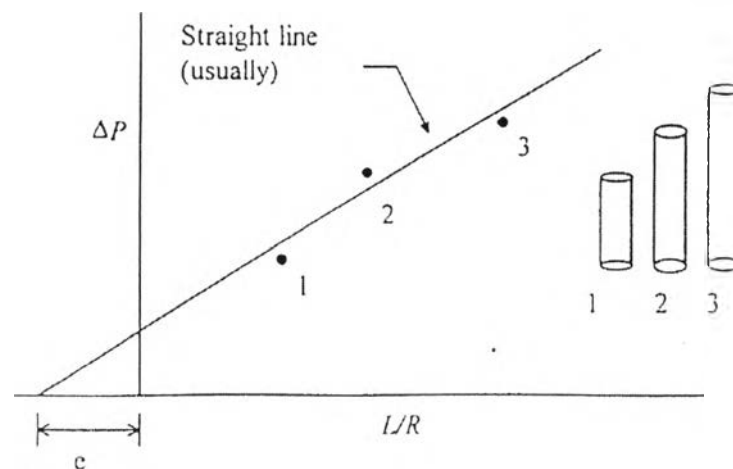

Figure 2.22 The Bagley correction for capillary rheometer (Reprinted from Brydson, 1970).

As mentioned previously, the shear stress of Equation (2.16) becomes

$$\tau = \frac{R\Delta P_{total}}{2L} \tag{2.19}$$

when $\quad \Delta P_{total} = \Delta P_{ent} + \Delta P_{cap} + \Delta P_{ex} = \Delta P_{cap} + \Delta P_{ends}$ (2.20)

and $\quad \Delta P_{cap} = \dfrac{2\tau L}{R}$ (2.21)

Define end correction $\quad e \equiv \dfrac{\Delta P_{ends}}{2\tau}$ (2.22)

Thus $\quad \Delta P_{total} = \dfrac{2\tau L}{R} + 2\tau e$ (2.23)

According to these corrections, the real shear stress is defined with Equation (2.24).

$$\tau_{real} = \frac{R\Delta P}{2(L + eR)} = \frac{\Delta P}{2\left(\dfrac{L}{R} + e\right)} \tag{2.24}$$

The Rabinowitsch correction is used to correct the shear rate at the wall. Since the shear rate varies across the radius of the capillary, hence, non-Newtonian fluids will have an effective viscosity that depends on radial position as shown in Figure 2.23.
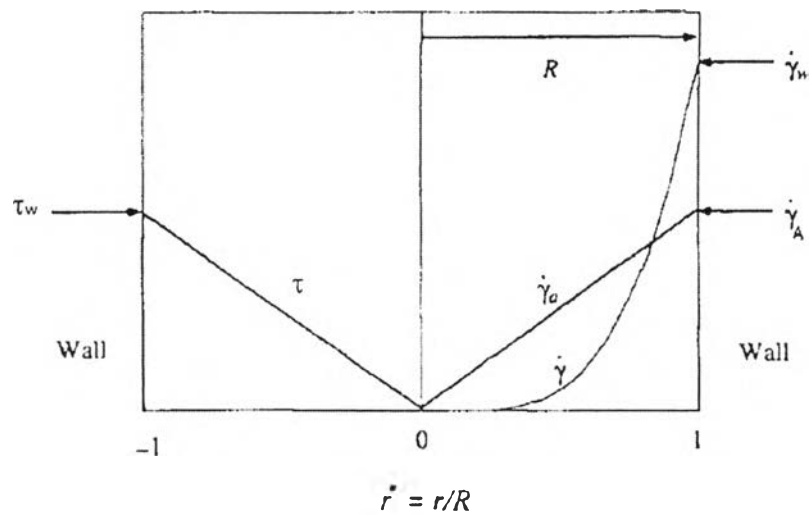
Figure 2.23 Dependence of real shear stress (τ) , apparent shear rate ($\dot{\gamma}_{app}$), and real shear rate ($\dot{\gamma}$) on radial position for a non-Newtonian fluid flowing in capillary (Reprinted from Nielsen, 1977).

This correction calculates the real wall shear rate from the apparent wall shear rate as shown in Equation (2.25).

$$\dot{\gamma}_{real} = \frac{3n'+1}{4n'} \dot{\gamma}_{app} \tag{2.25}$$

where n' is the slope from a plot (in a double logarithmic scale) between the apparent shear rate and the apparent shear stress.

According to these corrections, the real shear viscosity (η_{real}) of non-Newtonian fluids can be calculated by using the Equation (2.26).

$$\eta_{actual} = \frac{\tau_{actual}}{\dot{\gamma}_{actual}} \tag{2.26}$$

2.5.3 Temperature

Most polymers show the change in viscosity with temperature. For Newtonian fluids and for polymeric fluids at temperature far above the glass transition temperature or the melting point, the temperature dependence of shear viscosity affecting the flow activation energy of the material is observed using the Arrhenius-Frenkel Eyring Equation seen as Equation (2.27).

$$\eta = A_0 \exp\left(\frac{E_a}{RT}\right) \tag{2.27}$$

where η is the shear viscosity at a given shear rate, A_0 is approximately a constant, E_a is the flow activation energy, R is the molar gas constant, and T is the absolute temperature. The flow activation energy is related to the movement of molecular chain against the internal flow resistance caused by the friction between neighboring molecules, and it is determined by the slope of plots between ln η *versus* the reciprocal of temperature (1/T). The flow activation energy not only describes the energy needed for the molecular chains to move, but also provides valuable information on the sensitivity of the material towards the change in temperature. The higher the flow activation energy, the more is the temperature sensitivity of the material.

2.5.4 Shear Rate, Viscosity Ratio and Capillary Number

Most of polymeric materials (non-Newtonian fluids) show Pseudoplastic (shear-thinning) behavior that their viscosities decreased with increasing shear rate. For pseudoplastic behavior, asymmetric molecular chains are randomly oriented and/or extensively entangled at rest. Under low shear rate, these chain entanglements impede severely the flow of the melt. As a consequence, the shear viscosity of the blends is still high. The molecular chains are then disentangled by high shear rates, and they become oriented in the flow direction, resulting in the decrease of shear viscosity (Muksing *et al.*, 2008). This non-Newtonian behavior plays an important role in the processing and fabrication of plastics and elastomers.

Viscosity ratio (λ) is defined as the ratio of the viscosity of dispersed phase and the viscosity of continuous phase as shown in Equation (2.28).

$$\lambda = \frac{\eta_d}{\eta_c} \qquad (2.28)$$

when η_d is the viscosity of the dispersed phase (Pa.s) and η_c is the viscosity of the continuous phase (Pa.s). The viscosity ratio affecting the shape of dispersed phase in shear field for Newtonian fluids is shown in Figure 2.24. At higher rates of shear, the deformed drops of dispersed phase may either breakup into smaller drops or stretch out into long filaments (Rumscheidt and Mason, 1961). The spherical shape of the dispersed phase is found when the viscosity ratio is unity. Furthermore, there is less breakup and more filament formation as the λ increases. However, for polymeric fluids, the dispersed phase may not be spherical in shape and they have a greater tendency to form filaments. This is attributed to molecular chain entanglements preventing breakup by acting as temporary crosslinks. In other words, the elastic effect in polymer melts is prominent and causes the dispersed phase to elongate.
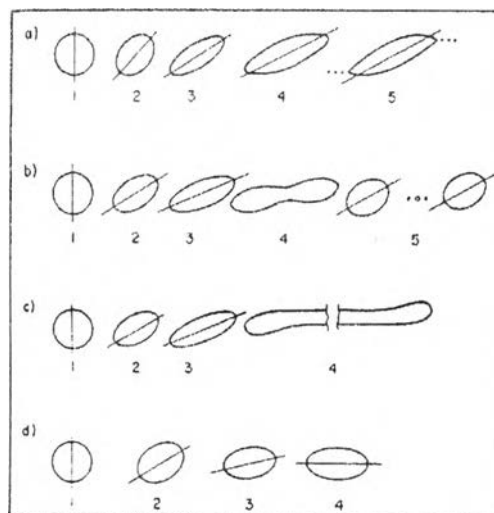

Figure 2.24 The dispersed phase shape in shear field as a function of shear rate from left (low shear rate) to right (high shear rate): a) λ = 0.0002, b) λ = 1.0, c) λ = 0.7, and d) λ = 6.0 (Reprinted from Rumscheidt and Mason, 1961).

The particle size of the dispersed phase is controlled by its dispersion. Hence, the relation of applied viscous force and counteracting interfacial force is significant. A dimensionless group that describes this relation is the Capillary number (Ca) and it can be expressed by Equation (2.29), so-called Taylor Equation (Taylor, 1934).

$$Ca = \frac{F_h}{F_c} = \frac{\eta_c \, \gamma \, R}{\sigma_{cd}}$$

(2.29)

where
F_h = hydrodynamic force

F_c = cohesive force of dispersed phased

η_c = viscosity of continuous phase

γ = shear rate

R = particle radius

σ_{cd} = interfacial surface tension

The combination of the continuous phase viscosity times shear rate describes the shear stress applied to the dispersed phase, and the particle radius is determined based on the surface energy of the polymer blend system. Under shear, the dispersed phase is elongated into a thread or ellipsoid or cylinder depending on their viscosity and concentration. During melt mixing, these elongated particles are still kept in the shear field, hence; the particles of the dispersed phase will begin to breakup due to the surface tractions. For the compatibilized blends, the compatibilization by addition of a third component or by in situ reactive blending leads to the increasing of interfacial adhesion between dispersed phase and continuous phase. The force on the surface of the dispersed phase exceeds the strength provided by its cohesive force, As a consequence, the elongated particles breaks and then forms spherical particles with uniform diameter. However, the droplet formation in the shear field is limited to the viscosity ratio of less than 3.5 (Grace, 1982). The droplet formation can be predicted from the product of a critical

capillary number (Ca$_{crit}$) times a function of the viscosity ratio as shown in Equation (2.30).

$$Ca_{crit} f(\lambda) = Ca_{crit} \frac{19\lambda + 16}{16\lambda + 16} = 0.16\lambda^{-0.6}$$ (2.30)

Figure 2.25 demonstrates the relationship between the critical capillary number *versus* the viscosity ratio. For $\lambda > 3.5$, stretching of a drop into a thread is impossible for shear flow due to a large difference in viscosities of the blend components. In addition, the critical capillary number only gives the information about the maximum drop size which can survive in a given flow in the absence of coalescence. It suggests that the most effective dispersion leads to the finest drop sizes, and this phenomenon occurs only when the viscosities of blend components are nearly matched. Comparing with the critical capillary number, for Ca < Ca$_{crit}$, a steady drop shape can be developed. However, if Ca > Ca$_{crit}$, the drop will be continually stretched until it breaks under the influence of interfacial tension.
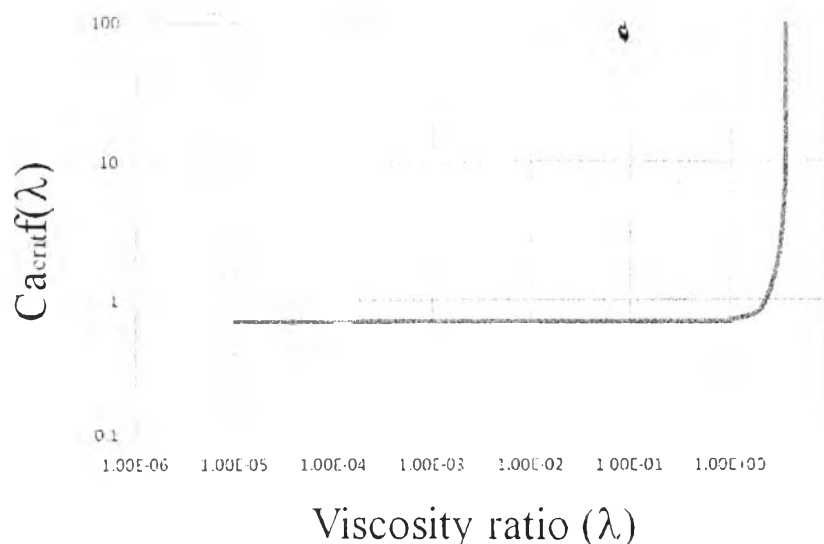

Figure 2.25 The critical capillary number as a function of viscosity ratio (Reprinted from Grace, 1982).

Back to Taylor Equation (2.29), using $Ca = Ca_{crit}$, the droplet diameter D can be calculated by using Equation (2.31).

$$D = \frac{2Ca_{crit}\sigma_{cd}}{\gamma\eta_c} \tag{2.31}$$

Later, Wu (1985) modified this Equation as seen in Equation (2.32)

$$D = \frac{4\sigma_{cd}\lambda^{\pm 0.84}}{\gamma\eta_c} \tag{2.32}$$

The exponent is positive for $\lambda > 1$ and negative for $\lambda < 1$. Serpe *et al.* (1990) further modified Wu Equation by using the blend viscosity rather than the matrix viscosity and by considering a term of composition (thus coalescence effects) as Equation (2.33).

$$D = \frac{4\sigma_{cd}(\eta_d/\eta_b)^{\pm 0.84}}{\gamma\eta_b[1-(4\phi_d\phi_c)^{0.8}]} \tag{2.33}$$

where η_b is the viscosity of the blend, and ϕ_d and ϕ_c are the volume fraction of the dispersed phase and the continuous phase, respectively. From these equations, it suggests that the size of dispersed particles is directly related to the interfacial tension between the two phases. The larger the interfacial tension, the less droplet will deform.

2.5.5 <u>Extrudate Swell</u>

The elasticity of polymer melt produces die swell or extrudate swell in the process of extruding a strand through a capillary. Generally, the elastic fluid is stretched by the shear field in the capillary and by the extensional flow field in the entrance region to the capillary (die) resulting in the orientation of molecular chains. When the melt emerges from the die, the forces are removed from the melt, hence; the recoiling of molecular chains occurs. This leads to the phenomenon of extrudate swelling as shown in Figure 2.26.
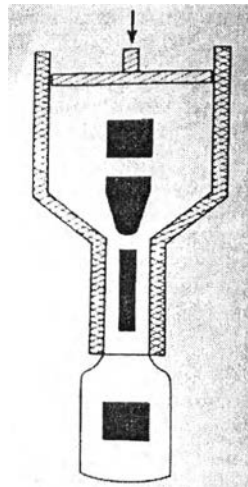

Figure 2.26 Extrudate swelling when the forces are removed at the end of the capillary (Reprinted from Nielsen, 1977).

The extrudate swell has an important role to play in polymer processing. The useful information of extrudate swell is used to control the size and shape of the extruded products for quality measurement, and to determine the productivity of the extruded products for quantity measurement. Factors affecting the extrudate swell are residence flow time, shear rate, die temperature, die length, etc. The decrease in die length and the increase in shear rate or shear stress are found to increase the extrudate swell. Hence, the extrudate swell can be minimized by increasing die temperature and die length or by reducing shear rate or shear stress.

2.6 Interparticle Distance

The interparticle distance (D_{ip}), surface-to-surface distance between two nearest rubber particles (see Figure 2.27), is directly proportional to the dispersed rubber phase diameter (D) and the reciprocal volume fraction of rubber (ϕ_r) as reported by Wu's model (1985) in Equation (2.34).

$$D_{ip} = D\left[\left(\frac{\pi}{6\phi_r}\right)^{1/3} - 1\right]$$
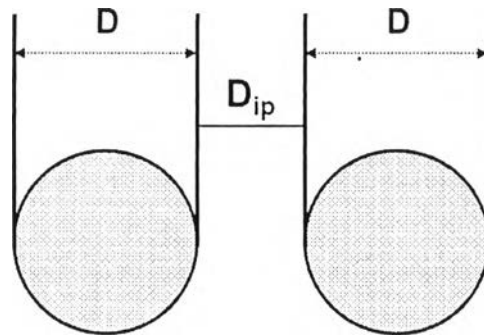
(2.34)

Figure 2.27 Model for (surface to surface) interparticle distance (D_{ip}) and rubber particle diameter (D).

The interparticle distance, referred to as the matrix ligament thickness, is a crucial morphological parameter which affects the toughening efficiency. In rubber-modified polyamides, the blends are super-tough if the rubber particle size (Huang *et al.*, 2004) and the interparticle distance (Wu, 1988; Harrats and Groeninckx, 2005) are less than 0.3 μm as shown in Figures 2.28 and 2.29, respectively.
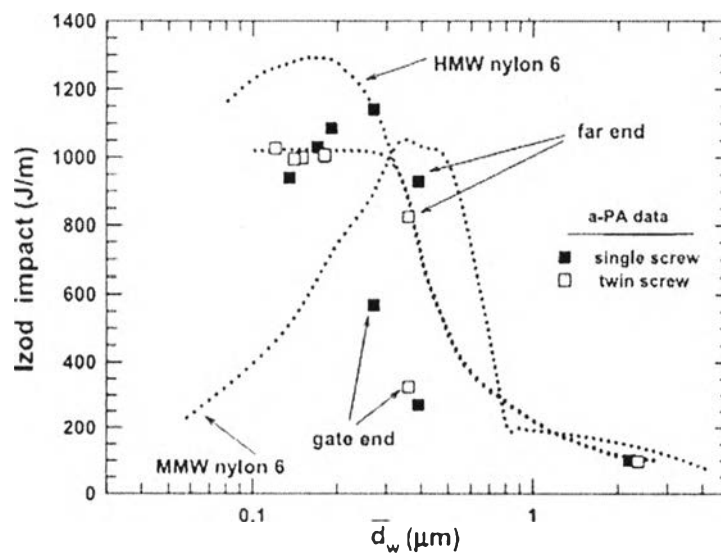
Figure 2.28 Effect of the weight average rubber particle size on room temperature Izod impact strength of Nylon6/SEBS/SEBS-g-MA blends containing 20 wt% total rubber content (Reprinted from Huang *et al.*, 2004).
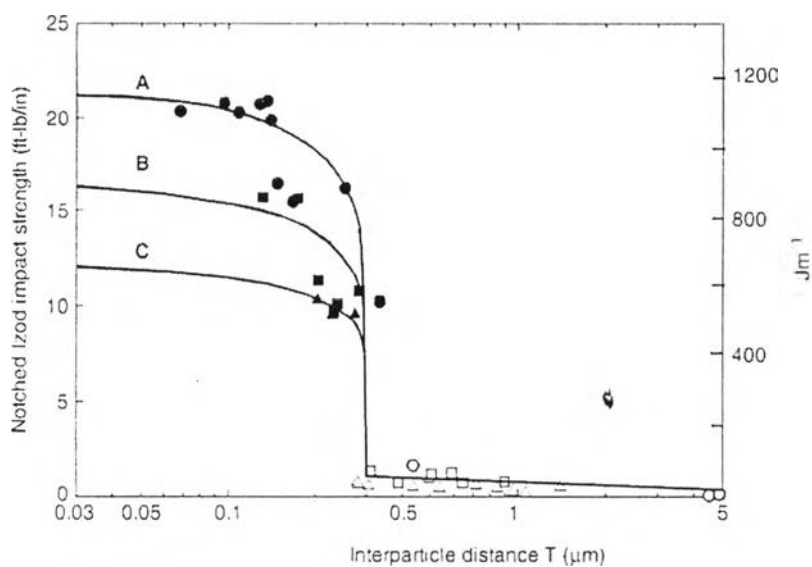

Figure 2.29 Notched Izod impact strength *versus* interparticle distance in Nylon6,6/ reactive rubber blends; curve A: 10 wt% rubber, curve B: 15 wt%, and curve C: 20 w% rubber (Reprinted from Harrats and Groeninckx, 2005).

For rubber toughening, the elastic modulus of the dispersed rubber phase is different from that of the polymer matrix. Thus, when a force is applied to a sample of the polymer/rubber blends, a stress concentration will form around particles of the dispersed rubber phase. Its scope can be described as a stressed volume, in which the diameter of the stressed volume (S) is defined as the sum of the interparticle distance and the dispersed phase diameter as shown in Equation (2.35) and Figure 2.30 (Margolina and Wu, 1988; Wu, 1990).
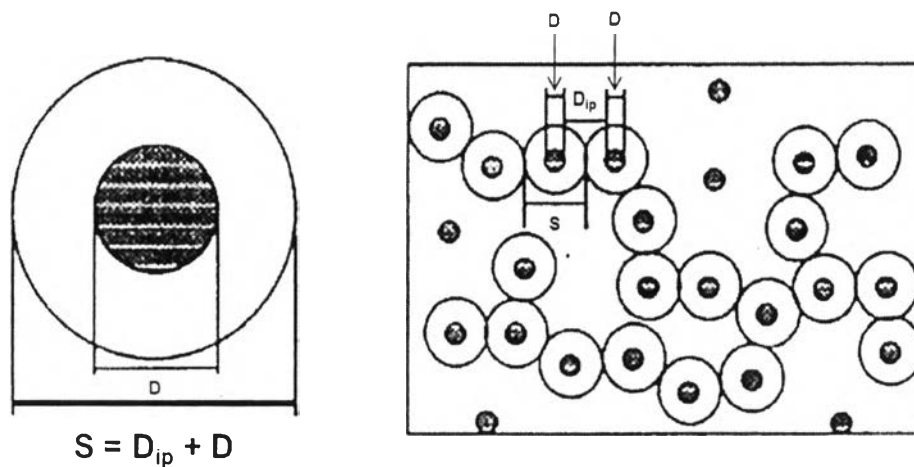
$$S = D_{ip} + D \tag{2.35}$$

Figure 2.30 Schematic diagram of stressed volume around a dispersed particle (Reprinted from Margolina and Wu, 1988).

During impact or tensile fracture of the polymer/rubber blends, the rubber particles will be greatly deformed until cavitation of the rubber particles occurs. The small rubber particles can suppress crazing and crack growth, and allow for stress fields overlapping around the adjacent rubber particles which results in shear yielding through matrix ligaments (Jiang et al., 1998). This behavior is necessary for toughening of semicrystalline polymers.

2.7 Literature Review

2.7.1 Rubber-toughened Plastics

Borggreve *et al.* (1987) stated that the impact energies of Nylon6 were affected by EPDM rubber concentration and particle size. The impact energies were greater when rubber content was increased and particle size was decreased.

Kumar *et al.* (1996) studied on the mechanical properties of Nylon-nitrile rubber blends having different plastic-rubber component ratios (100/0, 80/20, 70/30, 60/40, 50/50, 40/60, 30/70, 20/80, and 0/100). They revealed that the mechanical properties have a strong dependence on the amount of nylon in the blend. It is found that the blends with higher proportions of nylon have superior mechanical properties.

Phinyocheep *et al.* (2007) studied on the melt blending of PET/NR and they found that the toughness and impact strength of the PET/NR blend increased as the amount of NR was increased. This is due to the interaction between the carbonyl group of PET with the abnormal groups such as hydroxyl function in NR, resulting in improving the compatibility of PET/NR blend, hence increasing the toughness.

Tanrattanakul *et al.* (2008) focused on the use of epoxidized natural rubber (ENR) as a toughening agent for Nylon6 (PA6). The increasing of ENR content increased impact strength and elongation at break but decreased yield stress and tensile strength of PA6. These results showed that the rubber particle size increased as the concentration of ENR increased, leading to a reduction in tensile properties. However, rubber concentration, not rubber diameter, plays a major role in impact strength, or PA6/ENR blends may not require submicron particles for high toughness.

2.7.2 Effect of Compatibilization on Blend Morphology and Blend Properties

Otterson *et al.* (1991) studied the influence of styrene-acrylonitrile-maleic anhydride terpolymers (SANMA) used as a compatibilizer on the morphology and mechanical properties of a blend of Nylon6 and ABS. The results showed that

the morphological domain size decreased significantly while the impact strength increased with increasing compatibilizer level up to 6 wt% as shown in Figure 2.31.
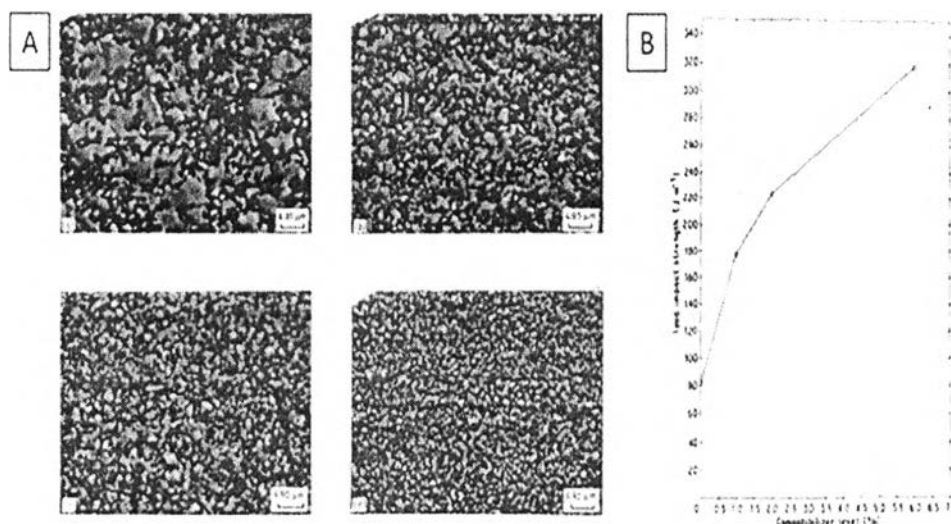

Figure 2.31 SEM micrographs (A) and Impact strength (B) of Nylon6/ABS binary blend and Nylon6/ABS/SANMA blends with various compatibilizer levels.

Oshinski *et al.* (1992) reported that in Nylon6/[SEBS-g-MA] using nylon6 80 wt% and varying the weight ratio between SEBS/SEBS-g-MA, the particle sizes of dispersed phase were varied from 0.05 to 5 µm. The particle size decreased with increasing SEBS-g-MA composition. Only, the particle sizes in the range of 0.1–1 µm showed higher Izod impact strength than those having upper or lower size.

Bonner and Hope (1993) had investigated the reactive blending of maleic anhydride-graft-nitrile rubber (MA-g-NBR) and Nylon6. The results indicated the improvement of impact strength of Nylon6 with addition of the unmodified NBR as shown in Figure 2.32. The impact strength of Nylon6 was further enhanced when NBR was functionalized with MA, giving the similar impact strength to the blend containing the commercial additive (EPR-based polyamide). With decreasing testing temperature to -20°C, the Nylon6/MA-g-NBR showed the highest impact strength. This is probably due to the presence of a high level of grafted MA coupled with a relatively high degree of crosslinking in the MA-g-NBR.
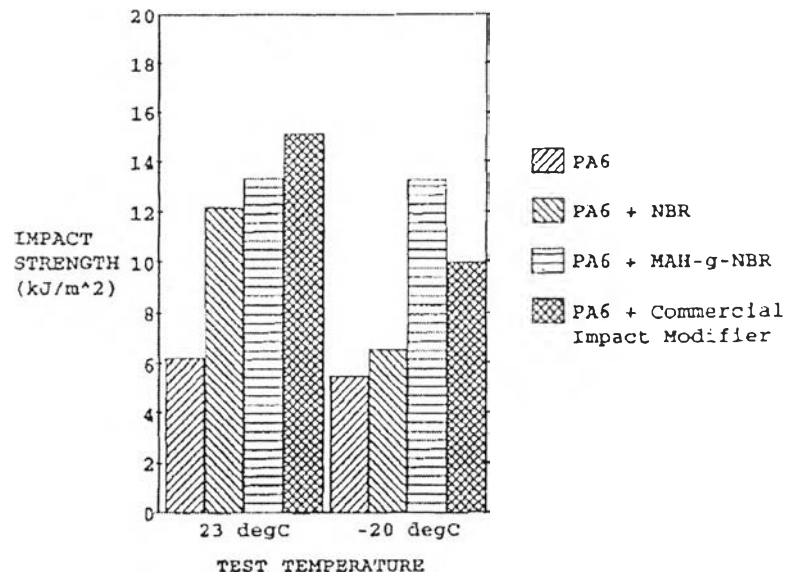
```
20
18
16
14
12                    ▨ PA6
IMPACT
STRENGTH 10           ▧ PA6 + NBR
(kJ/m^2)
8                     ▤ PA6 + MAH-g-NBR
6                     ▦ PA6 + Commercial
                         Impact Modifier
4
2
0
   23 degC   -20 degC
   TEST TEMPERATURE
```

Figure 2.32 Impact strength of Nylon6 blended with impact modifiers, revealing the effectiveness of MA-g-NBR at two different testing temperatures.

Tang and Huang (1994) showed that, when the compatibilizer used was either a block or graft copolymer, each was present at the interface and as micelles in matrix or dispersed phases. A greater quantity added only led to less effective participation as a compatibilizer. Moreover, at low concentration of the compatibilizer, each molecule occupies more interfacial area than at the higher concentration where the molecules arrange themselves more compactly in the interfacial area.

Park and Jo (1996) focused on the reactive compatibilization of immiscible PS/PA6 blends using PS modified with Maleic anhydride (MPS). The result showed that, although the content of MA in the MPS is low, the MPS acts effectively as a reactive compatibilizer. The compatibilizing ability of the MPS was very dependent on the molecular weight of the MPS. The high molecular weight MPSs were more effective in reducing and stabilizing the domain size of dispersed phase than the relatively low molecular weight MPS.

Horiuchi *et al.* (1997) studied the blends of PA6 and PC where PA6 is the continuous matrix. They found that the added maleated polymer (SEBS-g-MA and PS-MA) reacted with the amide end groups of PA6, and this interfacial reaction induced the change of the formation of the two dispersed phase from the stack formation to the capsule formation.

Schneider *et al.* (1997) studied the toughening of polystyrene (PS) by natural rubber (NR)-based composite particles. This work was focused on the influence of the morphology of composite NR-based particles on the toughness of PS. The results suggested that core-shell particle containing PS subinclusions in the rubber core are well suited for the toughening of PS. The hard shell assures adequate stress transfer at fast deformation speed and the rigid subinclusions render the rubber particles capable of stabilizing a generated craze since the incorporated rubber particles do not debond from the matrix.

Asaletha *et al.* (1998) reported that the addition of a graft copolymer of natural rubber and polystyrene (NR-g-PS) affected the rheological behavior of the natural rubber (NR)/polystyrene (PS) blend. The result was found that as the copolymer loading increases, the shear viscosity increases. This is due to the high interfacial interaction between the two components in the presence of the copolymer. The copolymer, in fact, locates at the interface and makes the interface broader. However, at higher loading of the copolymer, the viscosity of the blends decreases. This may be associated with the formation of micelles, which have a plasticizing action on the viscosity of the blends.

Jeon and Kim (1998) studied the 75/25 wt% poly(butlyterephthalate) and polystyrene (PBT/PS) blends showed that the dispersed phase diameter increased with annealing time and the irregular shape domain became spherical within 30 s in order to reduce the interfacial tension. When the PS-g-MA was added, the drop size decreased within a short time.

Asthana and Jayaraman (1999) revealed that a polymer reaction at the interfacial in reactively compatibilized polymer blends led to a reduction in particle size of the dispersed phase as well as a reduction in interfacial tension. Moreover, rheological observations showed that besides a reduction in interfacial tension, there

was an addition relaxation mechanism leading to enhancement in the storage modulus of the reactive blends as compared to the case of the nonreactive blends.

Agrawal *et al.* (2007) studied effect of different compatibilizers on the rheological, mechanical and morphological properties of Nylon6/PP (80/20 wt%) blends. The compatibilizers used were polypropylene grafted with 6 wt% of acrylic acid (PP-g-AA) and polypropylene grafted with 1 wt% of maleic anhydride (PP-g-MA). Torque rheometry analysis showed the increase in torque when PP-g-AA and PP-g-MA were added to Nylon6/PP blends, indicating that reactive compatibilization had occurred. For mechanical property, the impact strength of the blends containing PP-g-MA was greater than that of the blends containing PP-g-AA. Morphology observation showed that PP-g-MA improved considerably the adhesion between Nylon6/PP phases, leading to good mechanical properties.

Bordbar *et al.* (2007) studied toughness enhancement of Nylon6 and Nylon66 by using EPDM-g-MA and SEBS-g-MA. The results showed the ultra-toughened SEBS-g-MA blends, whereas EPDM blends under the same blending conditions did not show a significant improvement in toughness. Impact and tensile properties of the toughened blend with 20 wt% of SEBS-g-MA rubber showed about 1540 % improvement in impact and 240 % in elongation at break as compared with those of neat Nylon. It also related to morphological observations using SEM technique that revealed a co-continuous and a probable nano-scale-dispersed SEBS-g-MA in Nylon matrix.